Hydrol. Earth Syst. Sci. Discuss., 10, 9999–10034, 2013
www.hydrol-earth-syst-sci-discuss.net/10/9999/2013/
doi:10.5194/hessd-10-9999-2013


Hydrology and Earth System Sciences Discussions
Open Access



# Modeling insights from distributed temperature sensing data

**C. R. Buck**[1] **and S. E. Null**[2]

[1]Butte County Department of Water and Resource Conservation, Oroville, California, USA
[2]Department of Watershed Sciences, Utah State University, Utah, USA

Received: 17 June 2013 – Accepted: 13 July 2013 – Published: 1 August 2013

Correspondence to: C. R. Buck (cbuck@buttecounty.net)

Published by Copernicus Publications on behalf of the European Geosciences Union.

## Abstract

Distributed Temperature Sensing (DTS) technology can collect abundant high resolution river temperature data over space and time to improve development and performance of modeled river temperatures. These data can also identify and quantify thermal variability of micro-habitat that temperature modeling and standard temperature sampling do not capture. This allows researchers and practitioners to bracket uncertainty of daily maximum and minimum temperature that occurs in pools, side channels, or as a result of cool or warm inflows. This is demonstrated in a reach of the Shasta River in Northern California that receives irrigation runoff and inflow from small groundwater seeps. This approach highlights the influence of air temperature on stream temperatures, and indicates that physically-based numerical models may under-represent this important stream temperature driver. This work suggests DTS datasets improve efforts to simulate stream temperatures and demonstrates the utility of DTS to improve model performance and enhance detailed evaluation of hydrologic processes.


## 1 Introduction

Advances in instrumentation and monitoring techniques have made collecting temperature data easier and made data robust. This has provided opportunities to explore hydrological processes in greater detail and model them in new ways (Macfarlane et al., 2002; Moffett et al., 2008; Selker et al., 2006a; Tyler et al., 2009; Westhoff et al., 2011, 2007). Recent applications of Distributed Temperature Sensing (DTS) technology to hydrologic studies have opened up an exciting and rapidly expanding area of field research. DTS methods allow for temperature measurement with high spatial resolution (1 m resolution for up to a 1000 m cable) and temporal resolution (fractions of a minute) (Selker et al., 2006a; Tyler et al., 2009).

DTS technology has a variety of applications for environmental science, including soil moisture research (Steele-Dunne et al., 2010), exploration of snow thermal processes (Tyler et al., 2008), analysis of temperature anomalies in a saltmarsh tidal channel system (Moffett et al., 2008), deployment in a fumarolic ice cave to estimate flank degassing rates (Curtis and Kyle, 2011), leakage detection in sewer-storm water systems and dikes (Hoes et al., 2009; Khan et al., 2010), lake hydrology (Vercauteren et al., 2011), deployment in deep well boreholes for characterization of aquifer dynamics (Macfarlane et al., 2002; Yamano and Shusaku, 2005), atmospheric study of the stable boundary layer (Keller et al., 2011), and multiple applications in rivers to explore and quantify groundwater-surface water interactions (Fleckenstein et al., 2010; Lowry et al., 2007; Selker et al., 2006b; Slater et al., 2010; Vogt et al., 2010; Westhoff et al., 2011).

The potential to obtain stream temperature measurements continuously – from mainstem conditions to side channel or micro-habitat areas – provides opportunities to improve field and modeling studies. It can be useful to collect these data prior to or following simulation modeling. DTS data can help improve stream temperature modeling by providing high quality input and calibration data, and by identifying mixing zones where model nodes should be located at more frequent intervals. DTS can also be used to post-process model results to explore heating processes and temperature variability of micro-habitats relative to the mainstem. High-resolution measured data builds on previous modeling efforts by more accurately quantifying the range of measured thermal variability, estimating the rate of longitudinal heating as water moves downstream, or identifying thermal refugia from small springs or other inflows.

Only a few studies in the literature use DTS data to improve stream temperature model calibration, even though obtaining temperature data with spatial resolution of less than 1 m and temperature resolution of ±0.01 °C provides abundant data (Selker et al., 2006a; Tyler et al., 2009). Westhoff et al. (2007) use DTS data as input and to calibrate an energy-based temperature model of a first order stream in central Luxembourg. The temperature model is based on a series of well-mixed two meter length reservoirs and simulates seven days in April 2006. Model simulation of stream temperatures is compared to DTS temperature data. DTS measurements from this first order





HESSD
10, 9999–10034, 2013

stream were used in two other studies to calibrate, improve, or expand the energy balance model by adding instream rock clasts as heat storage zones and describing hyporheic exchange (Westhoff et al., 2010, 2011). Roth et al. (2010) used Westhoff et al.'s (2007), energy balance modeling approach, comparing modeled temperatures against measured DTS data to explore effects of varying riparian vegetation conditions on stream temperatures. Their application is in the Boiron de Morges River in southwest Switzerland over a three day period in August 2007.

The objective of this study is to show the utility and value of DTS data in recalibrating an existing temperature model for river temperatures over a multiple week study period, and to provide insights on hydrologic processes that can enhance model development and interpretation of modeled results. Our hypothesis is that DTS input data will improve model result accuracy. To date, studies have focused on short-term experiments exploring in-stream processes over a period of a week or less. The DTS dataset for the Shasta River in Northern California used in this study extends from mid-August to mid-October 2010. This period of time spans the transition from irrigation season to non-irrigation season and captures atmospheric changes that occur as summer transitions into fall. This research contributes to the literature by demonstrating the value of long-term DTS observations for model calibration and increased confidence in simulated temperatures. The methods and findings developed here can be applied to river management and assessment of habitat suitability by deploying DTS in reaches of interest for restoration or reaches with more complex temperature dynamics due to pools or inflows. DTS data also could be used with existing simulation results to post-process a more realistic range of variability in stream temperature not captured in simulation results.

We show the value of post-processing existing modeled stream temperature results to quantify micro-habitat and the range of variability in stream temperatures that are not captured by modeling. This has widespread applications because models do not have to be rerun. In fact, simulation results can be used to highlight promising locations for restoration or other changes, and DTS can be deployed to better measure temper-



HESSD
10, 9999–10034, 2013

atures or monitor changes. In this way, we show that DTS technology complements simulation modeling and can provide much greater benefit than simulation modeling with standard temperature logger protocols.

## 2 Site description

The Shasta River is the last tributary on the Klamath River before Iron Gate Dam, the lowest dam on the Klamath River (Fig. 1). Native salmonid populations in the Klamath Basin have declined due to low flow conditions, warm stream temperatures, and migration barriers (NRC, 2004). Restoring the Shasta River for native trout and salmon is a no-regrets action to ameliorate poor in-stream conditions and future dam decommissioning activities on the Klamath River (Null et al., 2010). Three species of salmonids, coho salmon (*Oncorhynchus kisutch*), fall-run Chinook salmon (*O. tshawytscha*), and steelhead trout (*O. giardneri*) are present in the Shasta River. Spring-run Chinook trout were extirpated with construction of Dwinnell Dam at river kilometer (RK) 65 (Moyle, 2002). Klamath Basin coho salmon belong to the Southern Oregon/Northern California Coast evolutionarily significant unit, which was listed as federally threatened by the National Marine Fisheries Service in 1997 (EPA, 1997). Coho salmon are the only listed salmonid species, although all trout and salmon fish populations have been drastically reduced compared to historical populations that reportedly exceeded 80 000 returning adults in the 1930s (NRC, 2004; DWR, 2008). Stream temperatures are one of the major factors limiting salmonid survival in the Shasta River (NRC, 2004).

The Shasta River originates in the Eddies Mountains of rural Northern California and flows across the Shasta Valley for approximately 95 km northwestward to the Klamath River, with a catchment area of 2070 km$^2$. The valley is bounded by the Scott Mountains to the west, Siskiyou Mountains to the north, and the Cascade Range to the south and east. In the rain shadow of Mount Shasta, the valley is a high desert environment with hot, dry summers and cool winters. Mean annual air temperature for 2010 was 11.3 °C. Annual mean precipitation varies considerably with elevation with a minimum of 33 to





HESSD
10, 9999–10034, 2013

38 cm in the low elevation areas of the valley (DWR, 2008). The diverse geology of the area influences the region's complex hydrology. Volcanic deposits make up much of the valley floor's surficial deposits and most prolific groundwater aquifers (DWR, 2008). Mount Shasta, an active Cascade volcano, contributes recharge to a highly productive aquifer characterized by preferential flow paths through basalt flows. Volcanic debris flow material (older than the basalt flows) is the result of a debris avalanche from Mount Shasta. It is composed of a block and matrix facies of volcanic rocks and fine sandy ash-rich material, respectively. Its chaotic deposition leads to a lack of internal structure and low permeability and is understood to serve as a boundary impeding groundwater flow from the basalt, therefore giving rise to numerous springs along the contact between the formations (DWR, 2008).

The lower Shasta River is sustained by significant baseflows from springs, most notably, the Big Springs Complex, which joins the mainstem at RK 54.246 (Fig. 2a) and contributes approximately 2.5 $m^3 s^{-1}$ to the Shasta River during the non-irrigation season and about 1.7 $m^3 s^{-1}$ during the irrigation season. Groundwater springs are an important source of cold water (12–14 °C) to the Shasta River, which is otherwise subject to atmospheric heating and cooling. During spring and summer, river temperatures exceed 20 °C (Null et al., 2010), which surpasses the thermal tolerance for salmonid species (Myrick and Cech Jr., 2001).

Mean annual discharge (years 1934–2010) near the mouth of the Shasta River is 5.18 $m^3 s^{-1}$, with a range of 2.21–10.3 $m^3 s^{-1}$. Mean daily discharge for 2010 (an above average year) exemplifies the pattern of peak snowmelt runoff and subsequently reduced flows during the irrigation season from April through September (Fig. 3).

Our study site is approximately 0.8 km of the mainstem Shasta River downstream of Dwinnell Dam and upstream of the confluence with Big Springs Creek (Fig. 2), RK 54.898–55.699. This stretch has an average slope of 0.0028 $m\,m^{-1}$. The course of the river in this area runs along the base of the debris flow and averages a width of 11.3 m. Basalt outcrops are dispersed along the Shasta River and several small groundwater seeps contribute small amounts of cold (∼ 14 °C) water. The flow rate, size, and prevalence of these seeps have not been quantified. Most stream flow in this stretch originates from snowmelt runoff and groundwater accretion upstream and small seeps along the course of the mainstem. Summertime flows are on the order of $0.71\,m^3\,s^{-1}$ or less during the irrigation season.

The complex spring hydrology and prevalence of coldwater seeps makes better measuring, simulating, and characterizing the thermal diversity of the Shasta River a priority. Previous simulation modeling has indicated that restoration could enhance coldwater habitat in this river (Null et al., 2010). While it is generally known that coldwater springs and seeps exist in this system and that they play a role in maintaining a stable thermal regime, it is not well understood how exactly they influence stream temperatures or the role they play for thermal refugia. High resolution temperature monitoring in the Shasta River can help to fill these information gaps and also provide better input data for calibrating stream temperature models.

## 3 Methods

### 3.1 Measurements

A 4 channel Sensornet Oryx DTS was deployed to measure stream temperatures. DTS systems send a laser light down an optical fiber and measure the Raman backscatter, whose intensity is related to the temperature of the optical fiber (Selker et al., 2006a; Tyler et al., 2009). The DTS data logger is enclosed in a weather proof shelter with a 3G compatible cell phone data link. 200 Watt solar panels with two 70 amp-hour deep discharge batteries provide power. In our application, the DTS recorded water temperature every meter along a 1 km cable every 5 min 17 August to 6 September and then every 15 min 6 September thru 12 October because quarter hour resolution is sufficient for the purposes of this study and reduces excessive data storage and transmittal. The location of the DTS system at the upstream end of the cable is hereafter referred to as the DTS Base Station (DTS-BS) (Fig. 2). The cable was secured with fence posts or rocks and typically rested a few inches above the river bed. Macrophyte growth in the Shasta River (Jeffres et al., 2009) made the cable difficult to see and protected it from direct solar radiation. Instrumentation also included an eKo-brand remote weather station that measured precipitation, solar radiation, wind speed, temperature and relative humidity. This weather station was located in the middle of an open damp grassy area 30 m east of the river and recorded atmospheric data every 15 min.

An ice bath, periodically maintained over the study period, and ambient bath were located at the DTS-BS and another ambient bath was at the end of the cable. These calibration baths housed 20–30 m of coiled fiber optic cable situated such that the cable did not touch the sides of the bath. A Hobo temperature logger with accuracy of ±0.2 °C for the 0–50 °C temperature range and a high resolution temperature probe from the DTS system was placed in the middle of the coil for cable calibration to account for signal attenuation and temperature offset (Tyler and Selker, 2009). The cable measured and recorded stream temperatures in the mainstem Shasta River from approximately RK 55.649 to 54.898, the side channel of Parks Creek Overflow (PCO), and at two small groundwater seeps on river left (Fig. 2). The cable was placed in PCO and the groundwater seeps to quantify thermal differences between them and the mainstem Shasta River.

### 3.2 Stream temperature model

The Tennessee Valley Authority's River Modeling System (TVA-RMS v.4) was used to simulate flow and stream temperature in the Shasta River for 21 August thru 9 October 2010 with an hourly time step. RMS is a one-dimensional longitudinal, physically-based numerical model composed of a hydrodynamics module (ADYN) and a water quality module (RQUAL) (Hauser and Schohl, 2002). ADYN solves equations for conservation of mass and momentum (St. Venant equations) using a four point implicit finite difference scheme with weighted spatial derivatives outputting velocity and depth at each node. Required inputs include channel geometry, roughness coefficients, upstream and lateral inflows, and initial conditions specified as either flow or water sur-





HESSD
10, 9999–10034, 2013



C. R. Buck and S. E. Null

face elevation (Hauser and Schohl, 2002). The dynamic water quality model (RQUAL) solves the mass transport equation using the Holly–Priessmann numerical scheme and can simulate time varying temperature, dissolved oxygen, carbonaceous BODu, and nitrogenous BODu at multiple locations (nodes) along a river reach. Modeling temperature was the focus of this study, and the other water quality aspects were not simulated. Model inputs for RQUAL include velocity and water surface elevation from ADYN, meteorological data (air temperature, dew point temperature, wind speed, cloud cover, barometric pressure, and solar radiation), temperatures of inflow sources, and initial stream temperatures (Hauser and Schohl, 2002).

The temperature component of the water quality module uses a heat budget approach estimating heat fluxes for net solar radiation adjusted by a shading factor, atmospheric long-wave radiation, channel bed heat flux, back radiation from the river, evaporative heat loss, and conductive heat transfer (Hauser and Schohl, 2002). Changes to the RMS code to represent riparian shading were made by Abbot (2002) allowing for a separate shading fraction for the left and right bank of a river.

Meteorology input data for RQUAL (dry bulb temperature, atmospheric pressure, wind speed, solar radiation and relative humidity) were obtained from the eKo-brand weather station located near the river. Dew point temperature was calculated from dry bulb temperature and relative humidity. Cloud cover was estimated using measured short wave solar radiation.

Modeling efforts for this study began with a previously developed RMS model of the Shasta River simulating temperatures from Dwinnell Dam to the confluence with the Klamath for 2001 (Null et al., 2010). That model represented the Shasta River with 999 unevenly-spaced nodes over a modeled length of 65.4 km. Meandering reaches, as in the currently modeled section, have a higher density of nodes than straighter reaches (Fig. 2). The approximately 0.8 km fiber optic cable placed in the mainstem in summer 2010 corresponds to eleven of the nodes from the 2001 model. A five-point channel cross-sectional geometry defines each node. The new Shasta River model





HESSD
10, 9999–10034, 2013

for 2010 has a boundary condition node and 11 nodes modeling stream temperature, representing approximately 0.72 km.

The most upstream RMS node (node 0) is assigned boundary condition temperature and flow inputs and in the 2010 model is located upstream of the DTS stretch (Fig. 2). A Hobo temperature logger located about 40 m downstream of the boundary condition node (node 0) but upstream of the DTS cable provided hourly upstream boundary condition temperature data.

### 3.3 Calibration

Modeled water temperature was compared to DTS measured data averaged over 15–50 m upstream and downstream of each node. This was done rather than taking temperature at a single point closest to the model node to avoid capturing localized temperature conditions of the cable at a single location. This is important because the DTS cable captures spatial variability that is not represented with the model. Averaging measured temperature over space better represents water temperature conditions corresponding to each modeled reach.

Mean bias is calculated for each node by averaging the difference between hourly modeled and measured temperature for the model period, 21 August to 9 October. A positive mean bias indicates overestimation by the model. Similarly, the root mean square error (RMSE) is calculated for the same hourly time series by averaging the squared residuals (absolute value of modeled minus measured) and taking the square root.

## 4 Results and discussion

This section describes the model calibration process and results followed by DTS temperature results. Daily thermal variability of measured and modeled stream temperatures are also presented and discussed. Finally an examination of longitudinal heating for measured vs. modeled results explores the roles of solar radiation and air temperature on stream temperatures.

### 4.1 Boundary condition calibration

We explored the sensitivity of stream temperatures to the upstream flow boundary condition, as well as the inflow of Parks Creek Overflow (PCO) during calibration since these flows were estimated rather than measured. Overall, temperatures were not highly sensitive to the upstream flow boundary condition. The order of change to modeled stream temperatures was thousandths of a degree (°C) and the largest improvement from one model run to another was a mean bias of 0.039 °C. Changing the upstream inflow within its likely flow range has negligible effects on river temperature. A new lateral flow (not included in the 2001 RMS model) was added at node 9 to represent the inflow of PCO. PCO may be an abandoned channel of Parks Creek, but now is a narrow, rocky channel with dense vegetation that mostly conveys tail water return flow from flood-irrigated pasture. Flow data for this lateral was unavailable, but was estimated to be 0.05 to 0.11 $m^3 s^{-1}$ based on five flow measurements taken above and below the inlet. We believe the inflow of PCO varies based on irrigation events. During calibration, models were run with uniform daily flows of 0.06 to 0.14 $m^3 s^{-1}$. Based on model performance and knowledge of the river system, a uniform daily flow rate of approximately 0.11 $m^3 s^{-1}$ was assigned to PCO lateral. Lack of flow data for this inflow is a limitation and may affect downstream temperatures. For nodes 10–11, changes in the lateral flow from 0.06 to 0.14 $m^3 s^{-1}$ affects the mean bias on the order of a tenth of a degree (°C) and the RMSE as much as 0.058 °C. Boundary condition inflow temperatures for PCO were an average of temperatures along 15 m of DTS cable looped into the side channel.

A number of inputs were adjusted slightly from 2001 RMS model values for model calibration and are still within the recommended range (Hauser and Schohl, 2002) (Table 1). These included bank width, the wind coefficient in wind-driven evaporative cooling (AA), thermal diffusivity of bed material (DIF), and bed albedo (BEDALB). Other parameters, including bed heat storage capacity, effective channel bed thickness of the upper layer for bed heat conduction, wind exponent in wind-driven evaporative cooling, and the light extinction coefficient (CV, XL, BB, EXCO, respectively), were tested but either had little or no effect on modeled temperatures or worsened model performance.

## 4.2 Calibration results

Overall, modeled data represented stream temperatures in the Shasta River well. Modeled stream temperatures were compared with measured data (Fig. 4) and mean bias, root mean square error (RMSE), and mean absolute error (MAE) statistics were calculated for each node. MAE is less than 0.3 °C for all nodes and mean bias for all nodes is −0.04 °C. 2001 RMS model results had MAE of 1.48 and 1.90 °C for nearby reaches (Parks Creek and Louie Road) (Table 2). Using DTS as input data and for calibration improved model performance considerably for this short reach (0.8 km) with a decrease of the RMSE from 2.00 to 0.35 °C from the earlier 2001 RMS model to the newly calibrated model and MAE improved by 1.19 °C. A couple degrees (°C) can be significant when evaluating the suitability of temperature conditions for fish habitat or ranking ecosystem management alternatives, and using DTS for initial stream temperature helps improve model accuracy. Model accuracy could not be further improved because DTS data captures spatial thermal variability which is not as well represented in the coarser resolution stream temperature model.

We compared measured and modeled river temperatures at node 4 for visual corroboration of results (Fig. 4). Daily minimum modeled temperatures of nodes 1–9 tend to be warmer than measured temperatures by approximately 0.2 °C. In other words, not enough cooling occurs at nighttime in model results. Modeled daily maximum temperatures for nodes 1–9 are warmer than measured temperatures about half the days by an average of 0.05–0.09 °C and cooler than measured temperatures by an average of 0.05–0.14 °C. Temperatures downstream of PCO (nodes 10 and 11) are strongly influenced by the inflow of that lateral and therefore are less accurate since flow volumes are uncertain (Table 2). Modeled maximum daily temperatures are warmer than mea-





HESSD
10, 9999–10034, 2013

sured temperatures at node 10 and 11 by approximately 0.3 °C, which occurs about 80 % of the days.

### 4.3 Measured temperature results

The DTS data show local thermal variability that was not evident from temperature simulation or from previous stream temperature measurements using thermistors located tens of kilometers apart. PCO and the two measured cold water seeps contribute water noticeably warmer and cooler, respectively, than the mainstem temperature (Fig. 5). The measured temperature range, calculated as the difference between maximum and minimum temperature for each meter along the cable over the period of record, shows sites with high and low temperature variability (Fig. 5a). The groundwater seeps are both consistently about 15.2 and 14.4 °C. Though significantly colder than the mainstem, these seeps do not contribute enough flow to affect mainstem temperatures significantly, although they could provide very localized thermal refugia for coldwater species. PCO is shallower than the mainstem with less thermal mass, and thus is colder than the mainstem at night and warmer during the day, with higher temperatures than the mainstem on average. Examining the range of temperature for each location along the cable is one way to identify groundwater inflows as they dampen diurnal temperature fluctuations. Aside from the two seeps, previously discussed, the dataset does not reveal significant groundwater inflows. Temperature affects from other seeps and any diffuse baseflow that may be occurring along the reach is not great enough or near enough to the DTS cable to influence the measured temperature. The warmer temperatures just downstream of PCO indicates a mixing zone where the PCO mixes with the mainstem and persists for about 40 m downstream of the PCO channel (Fig. 5). The length of the mixing zone would be expected to change with flow volume of both the mainstem and side channel. With DTS, we were able to specify stream temperatures, cold water seeps, and thermal variability of a side channel, and quantify the size of mixing zones in the Shasta River from the PCO return flow channel. This is useful for evaluating potentially beneficial thermal features or thermal barriers to fish passage.





HESSD
10, 9999–10034, 2013

Mean weekly maximum and mean weekly minimum stream temperatures are typically used as metrics for habitat suitability and fish survival (Welsh et al., 2001; McCullough, 1999). Temperature measurements using DTS allow for an evaluation of mean weekly minimum and maximum temperatures at a 1 m spatial resolution (Fig. 6). Thus, weekly metrics can be created with high spatial resolution and used to identify specific problem reaches or barriers to fish passage. One of the warmest sites in the study reach of the Shasta River is the mixing zone downstream of PCO inlet (Fig. 5), which reached a daily maximum of 24.15 °C during the study period. Although it has high daily maximum temperatures that may provide a thermal barrier during warm periods, this mixing zone cools sufficiently at night (average minimum of about 13 °C) thus would probably not prevent fish passage during the observed season. With detailed temperature data over space and time, potential thermal barriers can be better defined, and fitting restoration measures identified. For instance, the reach downstream of the PCO channel might be a promising reach to plant riparian vegetation to shade the channel and preserve cold temperatures from the cold water seeps. This could provide cover and thermal refugia for trout and salmon that hold until stream temperatures cool at night for fish to bypass the PCO confluence.

### 4.4 Daily thermal variability

Stream temperatures are driven by both source temperatures and response to atmospheric conditions. Thus both modeled and measured daily maxima and minima were influenced by atmospheric conditions. However, modeled stream temperatures were less variable than measured DTS temperatures (Fig. 7). The measurement period from mid-August to the first week in October had a combination of hot and milder days with maximum daily air temperature ranging from 15.4 to 36.9 °C (Fig. 8). DTS daily maximum river temperatures were generally warmer than modeled peak temperatures. Likewise, DTS daily minima were cooler than modeled daily minimum temperature. Therefore, not quite enough heating occurs during the day and not quite enough cooling at night in the model for most locations. This leads to lower thermal variability





HESSD
10, 9999–10034, 2013



C. R. Buck and S. E. Null

Title Page
Abstract | Introduction
Conclusions | References
Tables | Figures
◀| |▶
◀ ▶
Back | Close
Full Screen / Esc
Printer-friendly Version
Interactive Discussion

of modeled compared to measured temperatures for all nodes upstream of PCO. The average difference between modeled and measured daily thermal variability for nodes 1 to 9 is between 0.10–0.63 °C for 22 August thru 9 October.

Stream temperatures at nodes 10 and 11 located downstream of PCO are influenced by the contribution of this side channel and often modeled thermal variability (temperature range) is more extreme than measured (this occurs 41 out of 50 days). More accurate inflow data (rather than estimated constant flow value of 0.11 $m^3 s^{-1}$) would likely improve results. In reality, PCO inflow is not steady, but rather varies with tail water return. It is probable that input PCO inflow volume is too high on days that modeled thermal variability is more extreme than measured data. This illustrates why irrigation tail water (which is variable based on water rights, water availability, and watering schedules of multiple irrigators) can be challenging to model accurately. Furthermore the difference in volume between tail water return flow channels and the mainstem river means that return flows or other smaller channels typically heat and cool at different rates and thus can contribute warmer or cooler water based on season, time of day, and water year (wet years vs. dry years). The Shasta River is characterized by inflows of tail water returns and cool groundwater seeps and springs that are unquantified and often unmapped. This makes assessing habitat suitability difficult because modeled mainstem temperatures do not capture these local complexities. DTS technology allows measurement of thermal variability of these small micro-habitats. DTS data can be used to bracket the uncertainty and range of temperature that may occur in side channels, pools, and mixing zones of cool or warm inflows, or to gain more information on reaches that simulation modeling indicate may provide suitable habitat for coldwater species or are promising for restoration.

For example, the PCO mixing zone is influenced by inflow from the side channel and maximum and minimum temperatures significantly differ from mainstem temperatures just upstream. This thermally complex mixing zone is modeled with a single node (node 9). Maximum and minimum temperatures modeled at node 10 are compared to temperatures measured by DTS to explore the extent to which thermal variability differs due





HESSD
10, 9999–10034, 2013



C. R. Buck and S. E. Null

Title Page
Abstract | Introduction
Conclusions | References
Tables | Figures
◀| |▶
◀ ▶
Back | Close
Full Screen / Esc
Printer-friendly Version
Interactive Discussion

to the lateral inflow. Figure 9 shows maximum DTS temperatures can exceed modeled temperatures by as much as 5.6 °C. A difference of this magnitude could be significant in affecting the movement of coldwater species, like salmon and trout, though it is not captured by model results. Conversely, measured DTS daily minimum temperatures are less than modeled minimums by as much as 2.72 °C.

This demonstrates the utility of DTS data in providing insight on thermal variability of micro-habitats not simulated by modeling efforts. This could be important for analysis and application of modeling results used for evaluating habitat suitability. Analyzing the increased (or in cases of groundwater inflow, decreased) thermal variability resulting from local inflows can bracket the uncertainty of modeled temperatures.

### 4.5 Longitudinal rate of heating

Generally, river temperatures warm in the downstream direction when the atmosphere is warmer than water temperatures (summer and early autumn). Examining longitudinal heating shows how stream temperatures change as water moves downstream, and is a function of source inflows and temperatures, travel time, and atmospheric conditions. This is important for managing temperature for aquatic species because it identifies where heating occurs most rapidly and can highlight those areas for restoration (e.g., by planting riparian vegetation) or other management efforts to preserve cooler, upstream temperatures. Longitudinal rate of heating is calculated for DTS as the average of measured temperatures near node 8 minus the average temperatures near node 1 normalized by the distance between them (386 m). The same is done for RMS results for node 1 and 8. This stretch of river does not have known inflows affecting mainstem temperatures.

We focus on the rate of longitudinal heating of water temperatures between nodes 1 and 8 on 25–31 August; these six days span a period of higher to lower air (and corresponding water) temperatures and have a wide range in maximum daily solar radiation. Figure 10 shows the rate of longitudinal heating from DTS measured temperatures and RMS modeled temperatures with solar radiation (Fig. 10a) and air temperature





HESSD
10, 9999–10034, 2013

(Fig. 10b). Modeled temperatures are driven primarily by solar radiation, following current understanding of solar radiation as a major factor influencing both air and water temperatures (Johnson, 2003) and a major driver of heat energy flux (Caissie, 2006). Measured peak heating rates lag peak solar radiation by four to five hours (especially on days with high maximum solar radiation), and appear to more closely coincide with the timing of peak air temperature. Measured daily maximum stream temperatures also lag peak solar radiation by approximately the same amount of time. This observation that air temperature correlates well with stream temperature reinforces similar findings of other investigators (Mackey and Berrie, 1991; Mohseni and Stefan, 1999; Sahoo et al., 2009), although improving understanding of causation or driving factors is outside the scope of this research. Regardless, our results show that the heat balance approach used by the numerical model may overemphasize the influence of solar radiation or incorrectly represent the lag between solar radiation and stream temperature response, and fail to capture the full influence of air temperature on longitudinal rates of heating, particularly at night when modeled heating rates are significantly lower than measured heating.

These results suggest that high resolution measured stream temperatures, such as DTS datasets, are helpful for re-examining the assumptions of stream temperature drivers. Considerable research exists on air- and insolation-water temperature relationships (Caissie, 2006; Danehy et al., 2005; Mohseni and Stefan, 1999; Webb and Nobilis, 2007). Continuing research is needed to improve understanding of the role of air temperature and solar radiation in physically-based models, particularly at differing scales (stream temperature modeling at fine-, landscape-, or meso-scale may be driven by different processes and conditions). DTS datasets that provide abundant temperature data in space and time could be useful for exploring and calibrating such efforts.





HESSD
10, 9999–10034, 2013

## 5 Limitations

Modeling provides the opportunity to explore hydrological processes as well as management alternatives, yet any modeling effort has limitations. Necessary simplification of physical processes and river geometry are inherent limitations to modeling river temperature. These have been described in greater detail for the Shasta River model elsewhere (Null, 2008). For this study, an additional limitation is that upstream boundary condition data for the mainstem and Parks Creek Overflow (PCO) tributary were unavailable. Inability to develop a rating curve for mainstem flow due to excessive macrophyte growth and limited flow measurements introduced uncertainty in specifying the boundary condition for daily flow of the Shasta River. Although this affects the accuracy of the model to some degree, sensitivity analysis performed during model calibration show river temperatures are not very sensitive to this input. More importantly, DTS temperature data demonstrates that PCO inflow significantly affects downstream mainstem temperatures, therefore uncertainty in this inflow boundary condition reduces accuracy of modeled temperatures. This model could be further improved by measuring discharge for PCO and other small seeps that contribute flow to the mainstem and that may affect thermal variability.

Although DTS technology provides high resolution data spatially and temporally, it still has limitations in its ability to fully capture stream temperature dynamics. In this deployment, the DTS data is limited to capturing temperatures in a longitudinal transect upstream to downstream in the river and generally does not provide lateral stream temperatures. The cable placement also may vary with respect to its distance from the river bed. This makes it difficult to conclude with certainty that groundwater accretion does not occur at all within the monitored reach even though the data suggests that it does not, other than from the small observable seeps. However, a strength of DTS is its flexibility. Results from this deployment could further highlight locations of particular interest where cross-sections or coiling of the cable to measure temperatures in the water column could be done.





HESSD
10, 9999–10034, 2013

## 6 Conclusions

River temperature datasets using DTS technology provide a rich opportunity to explore and compare measured and modeled river temperatures, and to improve model performance and development, post-process existing modeled temperature results, and refine our understanding of processes governing stream temperature heat budgets. Using DTS data as input and to recalibrate the existing 2001 RMS stream temperature model for the Shasta River improved performance of modeled temperatures by reducing RMSE by almost 2.0 °C. Increasing confidence in simulated temperatures can make models more useful and effective for evaluating temperature conditions and therefore management alternatives. DTS data helps improve model performance by providing high quality input and calibration data.

DTS data-sets are also valuable for identifying and quantifying inflows and thermal variability from tail water, ungaged tributaries, side channels, and groundwater springs. DTS data helps identify mixing zones and in-stream thermal complexities to aide model node placement and frequency, thereby improving stream temperature model development. Side channels and groundwater seeps could be explicitly represented in future modeling studies if high resolution spatial data exits to define initial conditions, boundary conditions, and inform understanding of thermal dynamics.

Additionally, DTS data can be valuable for better interpreting existing simulation results. Deterministic stream temperature models most often solve a one-dimensional problem simulating temperatures longitudinally (Caissie, 2006). This means areas of increased thermal variability and complexity are not well captured in modeled temperature results, as explored by this work. Measured DTS data can be used with existing simulation results to post-process a more realistic range of variability in stream temperature, especially when simulation results are used to assess habitat suitability or management alternatives. In these cases, the details regarding timing and measured temperature variations are important. This will more realistically define potential thermal barriers to fish passage, thermal variability of micro-habitats, and more accurately





HESSD
10, 9999–10034, 2013

capture the variety of temperature conditions present in rivers. Collecting DTS data after model development has utility and value for post-processing modeled temperature results and understanding local thermal variability in relation to the mainstem temperature.

Analysis of longitudinal heating of measured vs. modeled temperatures revealed the overemphasis models such as RMS may place on solar radiation when estimating stream temperatures. This highlights the value of DTS data in revealing the strengths and weaknesses of heat budget representation in stream temperature models. Although research generally indicates solar radiation is the most important factor driving heat flux (Johnson, 2003), air temperature may still play a major role particularly with regards to the timing of longitudinal rates of heating and cooling or the timing of solar radiation heat transfer to streams may be currently mis-represented in models. Future work should further explore representation of solar radiation and air temperature in temperature models to improve model performance, longitudinal heating rates, and more accurately model the timing and magnitude of daily maximum and minimum stream temperatures. DTS data can help refine our understanding of processes governing stream temperature heat budgets.

*Acknowledgements.* The fiber-optic distributed temperature sensing instrumentation and expertise were provided by the Center for Transformative Environmental Monitoring Programs (CTEMPs) at the Oregon State University and the University of Nevada, Reno. Data collected will be available through the CTEMPs Data Services Program. CTEMPs operates as an Affiliated Instrument Node of CUAHSI and is supported by the National Science Foundation's Division of Earth Sciences Instrumentation and Facilities Program (EAR/IF) under Cooperative Agreements EAR-0929638 and EAR-0930061.





HESSD
10, 9999–10034, 2013

## References

Abbot, A. G. P.: The Effect of Riparian Vegetation on Stream Temperature in the Shasta River, Master's Thesis, U.C. Davis Dept. of Civil and Environmental Engineering, Davis, California, 2002.

Caissie, D.: The thermal regime of rivers: a review, Freshwater Biol., 51, 1389–1406, 2006.

Curtis, A. and Kyle, P.: Geothermal point sources identified in a fumarolic ice cave on Erebus volcano, Antarctica using fiber optic distributed temperature sensing, Geophys. Res. Lett., 38, L16802, doi:10.1029/2011gl048272, 2011.

Danehy, R. J., Colson, C. G., Parrett, K. B., and Duke, S. D.: Patterns and sources of thermal heterogeneity in small mountain streams within a forested setting, Forest Ecol. Manage., 208, 287–302, doi:10.1016/j.foreco.2004.12.006, 2005.

DWR: Shasta Valley, Siskiyou County Groundwater Data Needs Assessment (Draft), California Department of Water Resources, 2008.

EPA: Designated Critical Habitat, Central California Coast and Southern Oregon/Northern California Coast Coho Salmon, Federal Register: 62, 227, http://www.epa.gov/fedrgstr/EPA-SPECIES/1997/November/Day-25/e30865.htm (last access: July 2013), 1997.

Fleckenstein, J. H., Krause, S., Hannah, D. M., and Boano, F.: Groundwater-surface water interactions: new methods and models to improve understanding of processes and dynamics, Adv. Water Resour., 33, 1291–1295, doi:10.1016/j.advwatres.2010.09.011, 2010.

Hauser, G. E. and Schohl, G. A.: River Modeling System v4 – User Guide and Technical Reference, Report No. WR28-1-590-164, TVA River System Operations and Environment, Norris, Tennessee, 2002.

Hoes, O. A. C., Schilperoort, R. P. S., Luxemburg, W. M. J., Clemens, F., and de Giesen, N. C. V.: Locating illicit connections in storm water sewers using fiber-optic distributed temperature sensing, Water Res., 43, 5187–5197, doi:10.1016/j.watres.2009.08.020, 2009.

Jeffres, C., Dahlgren, R., Kiernan, J., King, A., Lusardi, R., Nichols, A., Null, S., Tanaka, S., and Willis, A.: Baseline Assessment of Physical and Biological Conditions Within Waterways on Big Springs Ranch, Siskiyou County, California, Report Prepared for: California State Water Resources Control Board, Davis, California, 2009.

Johnson, S. L.: Stream temperature: scaling of observations and issues for modelling, Hydrol. Process., 17, 497–499, 2003.





HESSD

10, 9999–10034, 2013

Modeling insights from distributed temperature sensing data

C. R. Buck and S. E. Null

Keller, C. A., Huwald, H., Vollmer, M. K., Wenger, A., Hill, M., Parlange, M. B., and Reimann, S.: Fiber optic distributed temperature sensing for the determination of the nocturnal atmospheric boundary layer height, Atmos. Meas. Tech., 4, 143–149, doi:10.5194/amt-4-143-2011, 2011.

Khan, A. A., Vrabie, V., Mars, J. I., Girard, A., and D'Urso, G.: Automatic monitoring system for singularity detection in dikes by DTS data measurement, IEEE Instrum. Meas., 59, 2167–2175, 2010.

Lowry, C. S., Walker, J. F., Hunt, R. J., and Anderson, M. P.: Identifying spatial variability of groundwater discharge in a wetland stream using a distributed temperature sensor, Water Resour. Res., 43, W10408, doi:10.1029/2007wr006145, 2007.

Macfarlane, P. A., Forster, A., Merriam, D. F., Schrotter, J., and Healey, J. M.: Monitoring artificially stimulated fluid movement in the Cretaceous Dakota aquifer, western Kansas, Hydrogeol. J., 10, 662–673, doi:10.1007/s10040-002-0223-7, 2002.

Mackey, A. P. and Berrie, A. D.: The prediction of water temperatures in chalk streams from air temperatures, Hydrobiologia, 210, 183–189, doi:10.1007/bf00034676, 1991.

Moffett, K. B., Tyler, S. W., Torgersen, T., Menon, M., Selker, J. S., and Gorelick, S. M.: Processes controlling the thermal regime of saltmarsh channel beds, Environ. Sci. Technol., 42, 671–676, doi:10.1021/es071309m, 2008.

Mohseni, O. and Stefan, H. G.: Stream temperature air temperature relationship: a physical interpretation, J. Hydrol., 218, 128–141, doi:10.1016/s0022-1694(99)00034-7, 1999.

Moyle, P.: Inland Fishes of California: Revised and Expanded, University of California Press, Berkeley and Los Angeles, 2002.

Myrick, C. A. and Cech Jr., J. J.: Temperature Effects on Chinook Salmon and Steelhead: a Review Focusing on California's Central Valley populations, University of California Press, Davis, CA, 2001.

NRC: Endangered and Threatened Fishes in the Klamath River Basin Causes of Decline and Strategies for Recovery, edited by: Council, N. R., National Academies Press, Washington, D.C., 2004.

Null, S. E.: Improving Managed Environmental Water Use: Shasta River Flow and Temperature Modeling, Ph.D., Geography Graduate Group, University of California, Davis, 195 pp., 2008.

Null, S. E., Deas, M. L., and Lund, J. R.: Flow and water temperature simulation for habitat restoration in the Shasta River, California, River Res. Appl., 26, 663–681, doi:10.1002/rra.1288, 2010.





HESSD

10, 9999–10034, 2013

Modeling insights from distributed temperature sensing data

C. R. Buck and S. E. Null

Roth, T. R., Westhoff, M. C., Huwald, H., Huff, J. A., Rubin, J. F., Barrenetxea, G., Vetterli, M., Parriaux, A., Selker, J. S., and Parlange, M. B.: Stream temperature response to three riparian vegetation scenarios by use of a distributed temperature validated model, Environ. Sci. Technol., 44, 2072–2078, doi:10.1021/es902654f, 2010.
Sahoo, G. B., Schladow, S. G., and Reuter, J. E.: Forecasting stream water temperature using regression analysis, artificial neural network, and chaotic non-linear dynamic models, J. Hydrol., 378, 325–342, doi:10.1016/j.jhydrol.2009.09.037, 2009.
Selker, J. S., Thevenaz, L., Huwald, H., Mallet, A., Luxemburg, W., van de Giesen, N., Stejskal, M., Zeman, J., Westhoff, M., and Parlange, M. B.: Distributed fiber-optic temperature sensing for hydrologic systems, Water Resour. Res., 42, W12202, doi:10.1029/2006WR005326, 2006a.
Selker, J. S., van de Giesen, N., Westhoff, M., Luxemburg, W., and Parlange, M. B.: Fiber optic opens window on stream dynamics, Geophys. Res. Lett., 33, L24401, doi:10.1029/2006GL027979, 2006b.
Slater, L. D., Ntarlagiannis, D., Day-Lewis, F. D., Mwakanyamale, K., Versteeg, R. J., Ward, A., Strickland, C., Johnson, C. D., and Lane, J. W.: Use of electrical imaging and distributed temperature sensing methods to characterize surface water-groundwater exchange regulating uranium transport at the Hanford 300 Area, Washington, Water Resour. Res., 46, W10533, doi:10.1029/2010wr009110, 2010.
Steele-Dunne, S. C., Rutten, M. M., Krzeminska, D. M., Hausner, M., Tyler, S. W., Selker, J., Bogaard, T. A., and de Giesen, N. C. V.: Feasibility of soil moisture estimation using passive distributed temperature sensing, Water Resour. Res., 46, 12, W03534 doi:10.1029/2009wr008272, 2010.
Tyler, S. W. and Selker, J.: New User Facility for Environmental Sensing, EOS, Transactions American Geophysical Union, 90, 483, doi:10.1029/2009EO500003, 2009.
Tyler, S. W., Burak, S. A., McNamara, J. P., Lamontagne, A., Selker, J. S., and Dozier, J.: Spatially distributed temperatures at the base of two mountain snowpacks measued with fiber-optic sensors, J. Glaciol., 54, 673–679, 2008.
Tyler, S. W., Selker, J. S., Hausner, M. B., Hatch, C. E., Torgersen, T., Thodal, C. E., and Schladow, S. G.: Environmental temperature sensing using Raman spectra DTS fiber-optic methods, Water Resour. Res., 45, W00D23, doi:10.1029/2008WR007052, 2009.





HESSD
10, 9999–10034, 2013

Vercauteren, N., Huwald, H., Bou-Zeid, E., Selker, J. S., Lemmin, U., Parlange, M. B., and Lunati, I.: Evolution of superficial lake water temperature profile under diurnal radiative forcing, Water Resour. Res., 47, 10, W09522, doi:10.1029/2011wr010529, 2011.

Vogt, T., Schneider, P., Hahn-Woernle, L., and Cirpka, O. A.: Estimation of seepage rates in a losing stream by means of fiber-optic high-resolution vertical temperature profiling, J. Hydrol., 380, 154–164, doi:10.1016/j.jhydrol.2009.10.033, 2010.

Webb, B. W. and Nobilis, F.: Long-term changes in river temperature and the influence of climatic and hydrological factors, Hydrolog. Sci. J., 52, 74–85, 2007.

Westhoff, M. C., Savenije, H. H. G., Luxemburg, W. M. J., Stelling, G. S., van de Giesen, N. C., Selker, J. S., Pfister, L., and Uhlenbrook, S.: A distributed stream temperature model using high resolution temperature observations, Hydrol. Earth Syst. Sci., 11, 1469–1480, doi:10.5194/hess-11-1469-2007, 2007.

Westhoff, M. C., Bogaard, T. A., and Savenije, H. H. G.: Quantifying the effect of in-stream rock clasts on the retardation of heat along a stream, Adv. Water Resour., 33, 1417–1425, doi:10.1016/j.advwatres.2010.02.006, 2010.

Westhoff, M. C., Gooseff, M. N., Bogaard, T. A., and Savenije, H. H. G.: Quantifying hyporheic exchange at high spatial resolution using natural temperature variations along a first-order stream, Water Resour. Res., 47, 13, W10508, doi:10.1029/2010wr009767, 2011.

Yamano, M. and Shusaku, G.: Long-term monitoring of the temperature profile in a deep borehole: temperature variations associated with water injection experiments and natural groundwater discharge, Phys. Earth Planet. In., 152, 326–334, 2005.





HESSD

10, 9999–10034, 2013

Modeling insights from distributed temperature sensing data

C. R. Buck and S. E. Null

**Table 1.** RQUAL parameters evaluated during calibration.

| Parameter | Recommended Range (Hauser and Schohl, 2002) | 2001 RMS (Null et al., 2010) | Current Value |
|---|---|---|---|
| AA[1] | 0E–09–4E–09 $m^3\,mb^{-1}\,s^{-1}$ | 0.5E–09 $m^3\,mb^{-1}\,s^{-1}$ | 0.2E–09 $m^3\,mb^{-1}\,s^{-1}$ |
| BB[2] | 1E–09–3E–09 $m^2\,mb^{-1}$ | 1.5E–09 $m^2\,mb^{-1}$ | 1.5E–09 $m^2\,mb^{-1}$ |
| DIF[3] | 25–50 $cm^2\,h^{-1}$ | 25 $cm^2\,h^{-1}$ | 50 $cm^2\,h^{-1}$ |
| XL[4] | 5–50 cm | 15 cm | 15 cm |
| EXCO[5] | 0.05 for clean water<br>0.30 for turbid water | 0.1 (1 $m^{-1}$) | 0.1 (1 $m^{-1}$) |
| CV[6] | 0.4–0.7 cal $cm^{-3}$ °C | 0.68 | 0.68 |
| BEDALB[7] | 0.1–0.5 (unitless) | 0.25 | 0.3 |

[1] AA wind coefficient in wind-driven evaporative cooling.
[2] BB wind exponent in wind-driven evaporative cooling.
[3] DIF thermal diffusivity of bed material.
[4] XL effective channel bed thickness of upper layer for bed heat conduction.
[5] EXCO light extinction coefficient.
[6] CV bed heat storage capacity.
[7] BEDALB albedo of bed material.





HESSD
10, 9999–10034, 2013



C. R. Buck and S. E. Null

**Table 2.** Calibration statistics at each node ($n$ = 1201 for all nodes).

| Node | Mean bias (°C) | RMSE (°C) | MAE (°C) |
|---|---|---|---|
| 1 | 0.04 | 0.14 | 0.11 |
| 2 | 0.03 | 0.15 | 0.12 |
| 3 | 0.05 | 0.14 | 0.11 |
| 4 | 0.02 | 0.15 | 0.12 |
| 5 | 0.00 | 0.15 | 0.13 |
| 6 | −0.02 | 0.17 | 0.14 |
| 7 | −0.06 | 0.18 | 0.15 |
| 8 | −0.11 | 0.21 | 0.17 |
| 9 | −0.16 | 0.24 | 0.19 |
| 10 | −0.10 | 0.30 | 0.24 |
| 11 | −0.16 | 0.35 | 0.29 |
| Average | −0.04 | 0.20 | 0.16 |
| Earlier 2001 RMS Model Results | | | |
| Parks Creek | −0.96 | 2.00 | 1.48 |
| Louie Road | −0.09 | 2.27 | 1.90 |





HESSD
10, 9999–10034, 2013

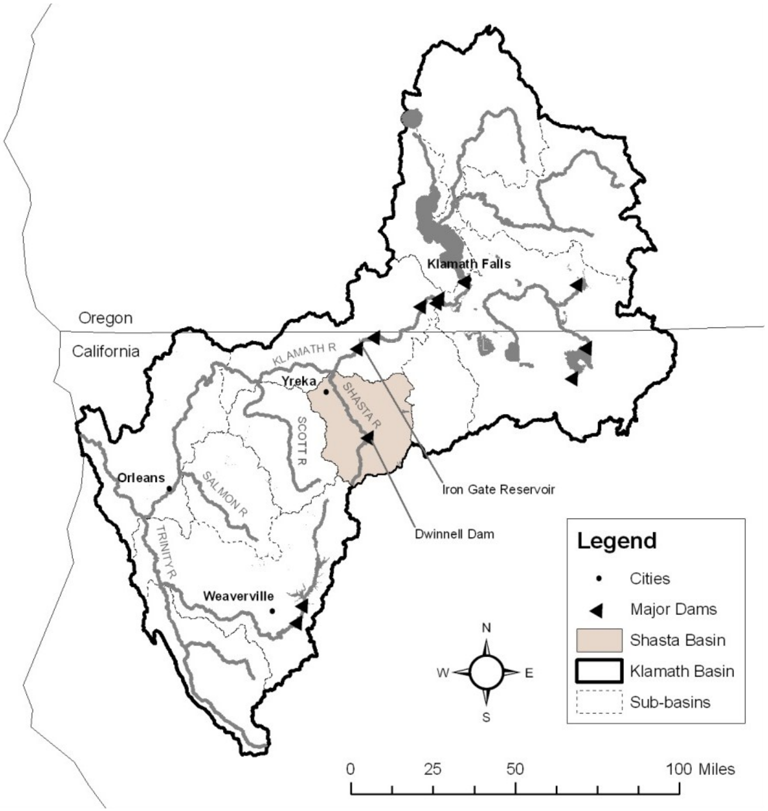


**Fig. 1.** Shasta River and Klamath River watersheds.





HESSD
10, 9999–10034, 2013



C. R. Buck and S. E. Null

A

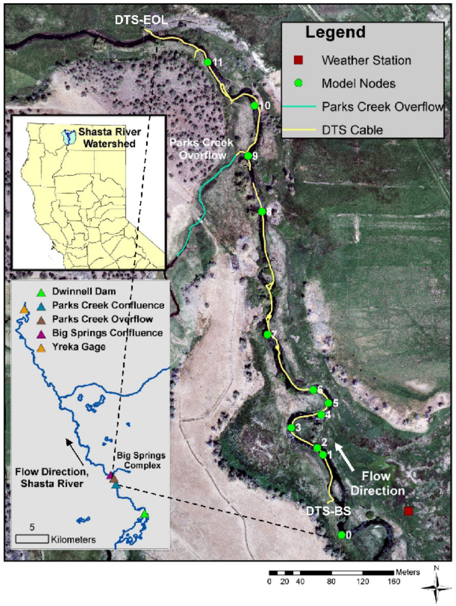


B

| River Kilometer | Approximate Distance from Upstream Node (m) | Description |
|---|---|---|
| 65.372 | | Dwinnell Dam |
| 56.229 | | Parks Creek Confluence |
| 55.699 | | RMS node 0, Upstream Boundary Condition |
| 55.659 | 40 | Hobo logger for boundary condition temperature |
| 55.649 | 50 | DTS cable enters river, near Base Station |
| 55.579 | 120 | DTS-BS flow cross section and stream gauge |
| 55.587 | 112 | RMS node 1 |
| 55.571 | 16 | RMS node 2 |
| 55.538 | 33 | RMS node 3 |
| 55.506 | 32 | RMS node 4 |
| 55.490 | 16 | RMS node 5 |
| 55.474 | 16 | RMS node 6 |
| 55.361 | 113 | RMS node 7 |
| 55.232 | 129 | Below Basalt Outcrop flow cross section |
| 55.200 | 161 | RMS node 8 |
| 55.136 | 64 | RMS node 9, Parks Creek Overflow Lateral |
| 55.130 | 6 | Parks Creek Overflow |
| 55.117 | 19 | Below Parks flow cross section |
| 55.056 | 80 | RMS node 10 |
| 55.038 | 18 | Groundwater seep2 |
| 54.975 | 81 | RMS node 11 |
| 54.960 | 15 | Groundwater seep1 |
| 54.898 | 77 | DTS- End of the Line (EOL), cable secured on fence post |
| 54.888 | 87 | EOL stream gauge and flow cross section |
| 54.246 | 729 | Big Springs Confluence |

Average distance between RMS nodes: 66 m

**Fig. 2. (A)** Shasta River DTS study area **(B)** descriptions of river kilometer locations (RMS is River Modeling System).





HESSD
10, 9999–10034, 2013

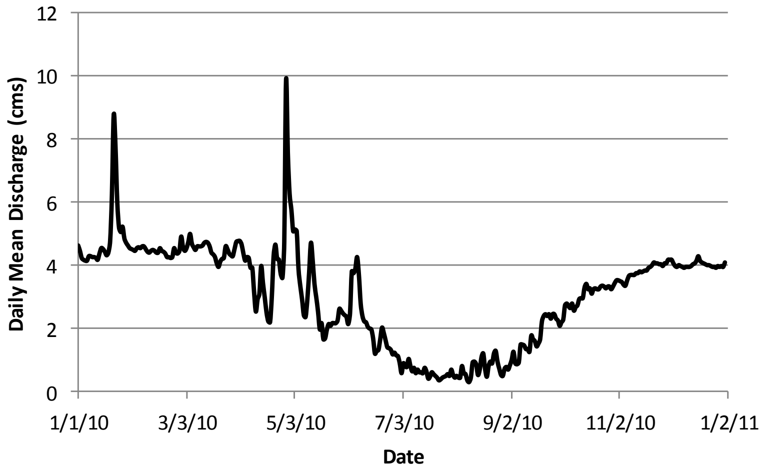


**Fig. 3.** Shasta River mean daily discharge ($m^3\ s^{-1}$) at USGS 11 517 500 gauge near Yreka.

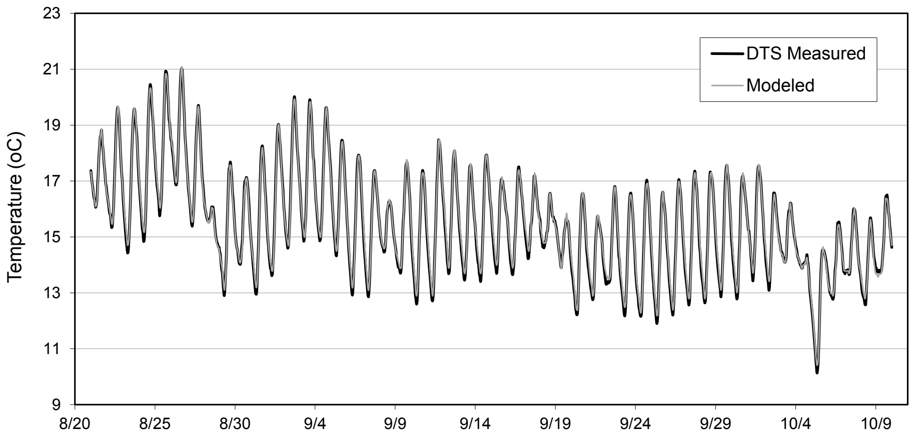


**Fig. 4.** Modeled and measured river temperature for node 4 with modeled temperature largely overlapping measured temperature except at the peaks and the troughs.





HESSD
10, 9999–10034, 2013

Modeling insights from distributed temperature sensing data

C. R. Buck and S. E. Null

Title Page
Abstract | Introduction
Conclusions | References
Tables | Figures
◀| |▶
◀ ▶
Back | Close
Full Screen / Esc
Printer-friendly Version
Interactive Discussion

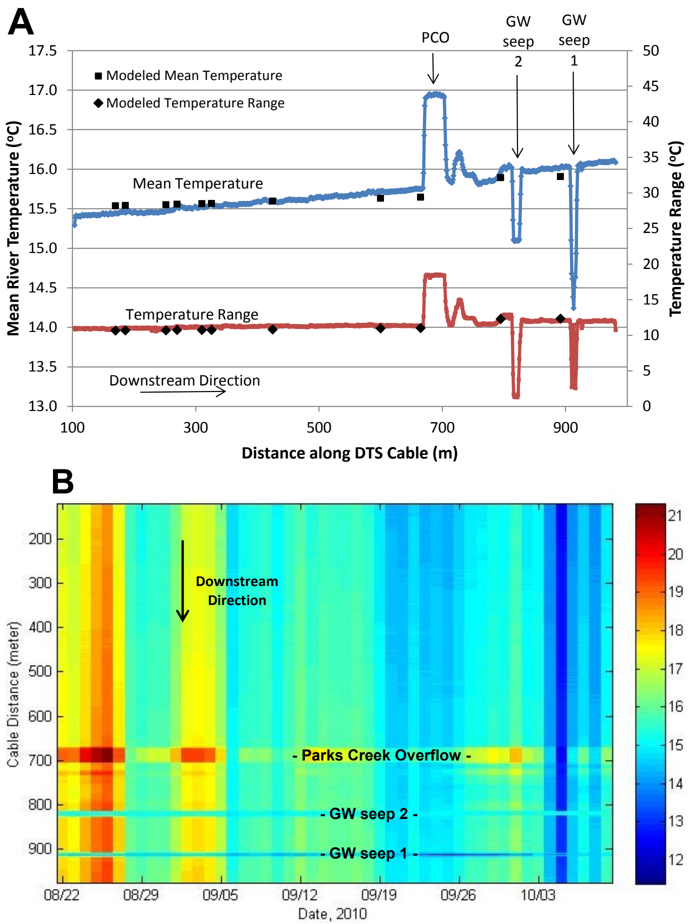


**Fig. 5. (A)** Longitudinal measured and modeled mean temperature and temperature range for measured period of record. **(B)** Mean daily temperature indicated by color ramp at meter increments along DTS cable for period of record.





HESSD
10, 9999–10034, 2013

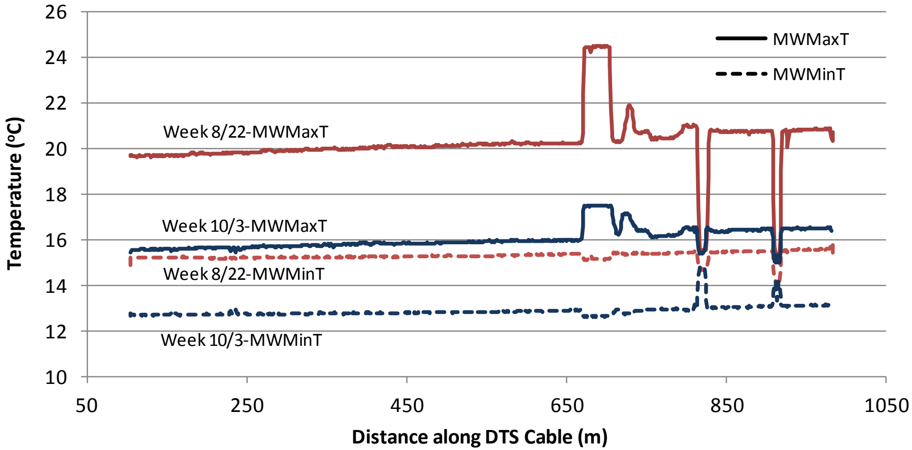


**Fig. 6.** Measured mean weekly maximum and minimum stream temperatures at each location for the hottest and coolest week.





HESSD
10, 9999–10034, 2013

Modeling insights from distributed temperature sensing data

C. R. Buck and S. E. Null

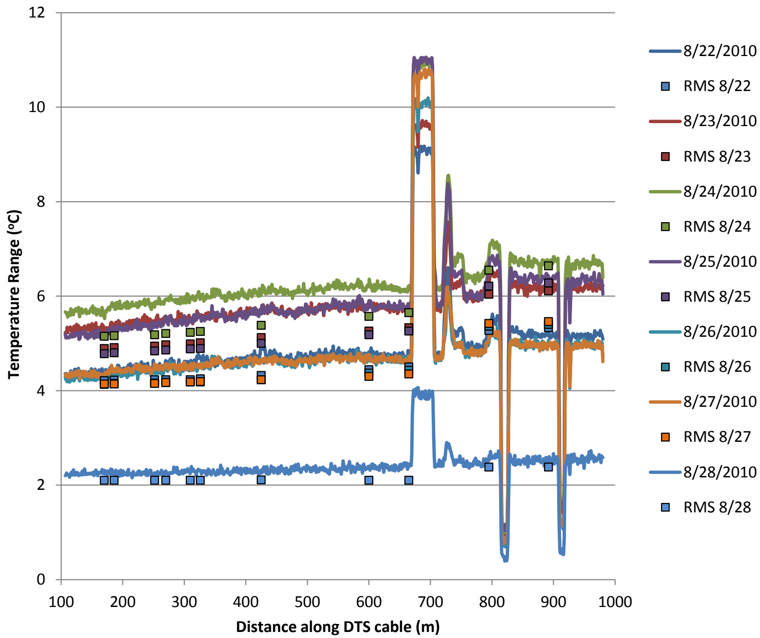


**Fig. 7.** Daily thermal variability of stream temperature (daily max–min) from DTS measured and modeled results for the week of 22 August.





HESSD
10, 9999–10034, 2013

Modeling insights from distributed temperature sensing data

C. R. Buck and S. E. Null

Title Page
Abstract | Introduction
Conclusions | References
Tables | Figures
Back | Close
Full Screen / Esc
Printer-friendly Version
Interactive Discussion

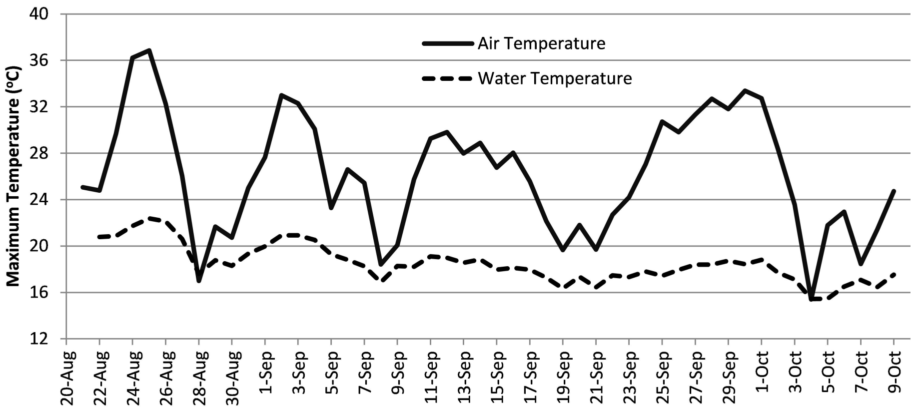


**Fig. 8.** Measured maximum daily air and water temperature for model period.





HESSD
10, 9999–10034, 2013

Modeling insights from distributed temperature sensing data

C. R. Buck and S. E. Null

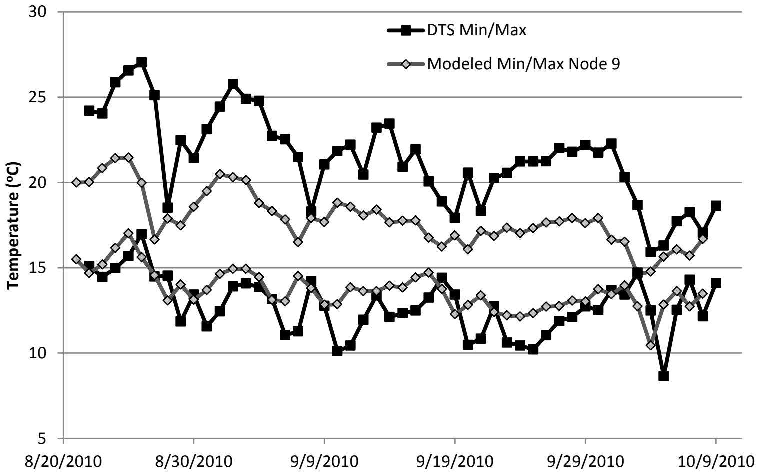


**Fig. 9.** Maximum and minimum modeled and measured temperatures in mixing zone of Parks Creek Overflow and mainstem Shasta River (node 9).





HESSD
10, 9999–10034, 2013

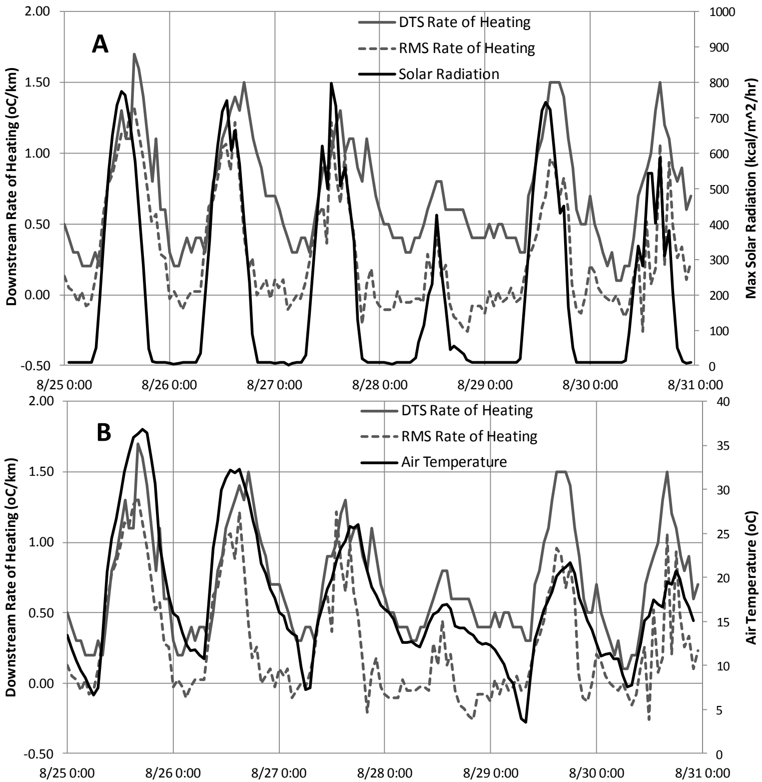


**Fig. 10. (A)** Hourly downstream rate of longitudinal heating (node 8 – node 1) with hourly solar radiation. **(B)** Hourly downstream rate of longitudinal heating (node 8 – node 1) with hourly air temperature.